

Development of antibacterial ZnO-loaded cotton fabric based on in situ fabrication

Xiao-Zhu Sun¹ · David H. Bremner² · Na Wan³ · Xiao Wang¹

Received: 16 June 2016 / Accepted: 3 October 2016 / Published online: 8 October 2016
© Springer-Verlag Berlin Heidelberg 2016

Abstract A method provided for the deposition of nanostructured ZnO on cotton fabric to introduce antibacterial functionality was presented in this article. This strategy enabled fabric to be coated with inorganic-based functional materials through in situ synthesis of nanoparticles using ultrasonic irradiation. The amino-terminated silicon sol (AEAPTS) was employed to generate nanostructured ZnO, and the mechanism of the ultrasound-assisted coating was proposed. Antibacterial activities, UV protection and other properties of ZnO-loaded cotton characterized by SEM, FTIR, XRD and TGA were investigated. The results indicated that ZnO-loaded cotton exhibited excellent UV protective property, efficient antibacterial activities, well water-resistant effect, together with moderate cytotoxicity against L929 and lower tensile strength. The developed method provides not only a facile way for in situ synthesis of ZnO on textile but also the production of antibacterial materials for healthcare applications.

1 Introduction

Antimicrobial finishing of textile fibers has attracted much attention in recent years [1–5] and has played a key role in the development of protective, decorative and functional

textiles. As a result, a large number of antimicrobial agents have been produced, and they can be broadly classified into two groups: organic and inorganic. Organic antibacterial materials are often less stable than inorganics particularly at high temperatures or pressures [6]. Inorganic materials containing metal and metal oxides such as silver or copper and a variety of metal oxides are increasingly popular due to their high surface area and durable activity [7, 8]. ZnO, regarded as a safe material for human beings and animals, are of particular interest because of the following properties: photocatalysis, UV protection and antimicrobial [9, 10]. ZnO nanoparticles, which can be prepared easily and cost effectively, have been used extensively in the formulation of personal care products [11]. Moreover, ZnO nanostructures present various biological applications due to their biocompatible nature such as controlling the growth of malignant cells. Antoine et al. [12] synthesized ZnO tetrapod nanoparticles and used them as microbicides to suppress HSV-2 genital infection in female BALB/c mice. Wahab et al. [13] investigated the role and toxicity mechanisms of ZnO nanostructures including nanoplates, nanorods, nanosheets and nanoflowers on cancer cells and fibroblast cells.

The common methods used for application of ZnO nanostructures on the fabric surface belong to cotton or polyester/cotton. Various approaches such as homogeneous precipitation [14], wet chemical [15] and hydrothermal methods [16] have been utilized for preparing ZnO-loaded cotton fabrics, which can be generally divided into a one-step process (in situ method) and a two-step process (ex situ method). Baruah et al. [17] applied one-step process to prepare nanowire ZnO on polyethylene fiber. The substrate was seeded by dipping fibers into concentrated ZnO colloidal solution and then heated to induce the growth of nanowire on the surface of fiber. The two-step process is

✉ Xiao-Zhu Sun
fathat@163.com

¹ School of Textile and Material Engineering,
Dalian Polytechnic University, Dalian 116034,
People's Republic of China

² School of Science, Engineering and Technology, Abertay
University, Kydd Building, Dundee DD1 1HG, Scotland, UK

³ ENO Biotechnology Co. Ltd, Dalian 116000,
People's Republic of China

more discussed in preparing ZnO-treated fabric due to its simplicity and compatibility. For example, Yadav et al. [18] fabricated nano-ZnO with a size of 40 nm by zinc nitrate and sodium hydroxide and attached it to cotton fabrics using acrylic binder. Mao et al. [16] applied ZnO nanoparticles synthesized by hydrothermal method to the SiO₂-coated fabric and the fastness against washing improved. The other method used for application of ZnO nanoparticles on the cotton fabric is known as layer-by-layer assembly [19]. The cationic cotton was soaked alternately in the anionic ZnO solution, deionized water and cationic ZnO solution until specific ZnO layers were deposited on the fabric surface.

Textiles are unstable at high temperatures or under harsh chemical environments, and the fabric texture is liable to be broke by plasma, irradiation or chemical agent used to fix nanoparticles onto the cotton fabric [20]. It is required to coat the nanostructure on them under gentle conditions and avoid causing surface defects or heterogeneity in layer thickness and composition. However, most of the preparation methods used for preparing ZnO-treated cotton fabrics involve high-temperature treatment, complicated technical process or expensive assistant composition. It is demanded for researchers to develop a green strategy for depositing ZnO on cotton fabrics under mild environment, and this method should exhibit good reproducibility, durability and homogeneity.

Herein, we demonstrate a simple, green and cost-effective silica-sol-based approach by which an effective antibacterial coating on cotton fabrics is achieved by growing ZnO on the substrate surface. The amino-contained sol and ultrasound are the key factors to mineralize and fabricate nanostructured ZnO in an aqueous medium under mild conditions. The method involves coating of cotton fabrics with AEAPTS sol followed by growth of nanostructured ZnO on the substrate from zinc precursors in an aqueous medium by use of ultrasound irradiation. The UV protective properties, antibacterial activities, cytotoxicity, washing stability and tensile strength of pure, AEAPTS-treated and ZnO-loaded cotton fabrics were investigated. ZnO-loaded samples were found with excellent UV protective property and antibacterial activity, together with moderate cytotoxicity.

2 Experimental

2.1 Materials

Zinc nitrate hexahydrate (Zn(NO₃)₂·6H₂O) were purchased from Sigma-Aldrich. Sol precursor, 3-(2-Aminoethylamino)propyltriethoxysilane (AEAPTS), was provided by Tcishanghai Co. Ltd. L929 mouse fibroblasts cells were

purchased from ENO biotech Co. Ltd. Scoured and bleached cotton fabrics (40 thread cm⁻¹ warp and 43 thread cm⁻¹ weft, 120 g/m²) were supplied by Dayao Textile. Hydrochloric acid (38 %), used as a catalyst, and other chemical reagents were of analytical grade and used as supplied.

2.2 Preparation of ZnO-loaded cotton fabric

The precursor AEAPTS silicon alkoxide was dissolved in a mixture of ethanol, water and HCl($n[\text{AEAPTS}]:n[\text{EtOH}]:n[\text{H}_2\text{O}]:n[\text{HCl}] = 1:8:50:8 \times 10^{-3}$). The solution was subsequently allowed to react at 35 °C for 4 h in a closed vial before applying to fabrics. A piece of dried cotton fabric was dipped in the sol solution with liquor-to-fabric ratio of 50:1(v/w) for 30 min with constant stirring. Then, the cotton fabrics were taken out and immersed in water containing zinc nitrate precursor(0.01 M) under ultrasonic irradiation for 30 min with a high intensity (25 kHz, 600 W) in order to allow the growth of ZnO on the cotton fabric surface. Finally, the treated samples were rinsed with water and dried at 60 °C in a laboratory oven for 2 h.

2.3 Characterization

The morphology of samples was analyzed by scanning electron microscopy (SEM) (JSM-5600LV, JEOL, Japan) equipped with an AZtec X-Max 20 system (EDS) for compositional analysis. Samples were gold-sputter-coated under argon prior to imaging.

The size and shape of ZnO nanoparticles were viewed at 80 kV with a JEM-2100 transmission electron microscope (TEM) (JEOL, Japan). To prepare the sample, a drop of the solution containing ZnO was placed onto a 400-mesh copper grid and dried at room temperature.

Fourier transform infrared spectroscopy (FTIR) was conducted in the attenuated total reflection mode using a Nicolet-Nexus 670 FTIR spectrometer (Nicolet Instruments, USA). Samples were analyzed by 12 scans with a 400–4000 cm⁻¹ scanning range and a resolution of 2 cm⁻¹.

X-ray diffraction (XRD) patterns were obtained on a D/MaxBR diffractometer (RigaKu, Japan) with Cu K α radiation (40 kV/30 mA) over the 2 θ range 10°–80°.

Thermogravimetric data were recorded on a TG209F1 thermogravimetric analyzer (TA Instruments, USA) from 20 to 900 °C at a heating rate of 10 °C/min under a nitrogen atmosphere.

ZnO content of samples was determined by ICP-MS on a Prodigy DRC spectrophotometer (Leeman, USA). The sample was prepared by dissolving it in HNO₃ (65 %) under microwave radiation, and the diluted solution was drawn to measure the concentration of ZnO.

2.4 Ultraviolet protection properties

Ultraviolet protection factor (UPF) and transmittance curves of the various samples were measured with a UV-1000F Labsphere Transmittance Analyzer (North Sutton, USA) using the EN 13758-1:2001 standard.

2.5 Antimicrobial testing

The antimicrobial activity of samples was estimated using ATCC 25922 method and shake flask method. Following the ATCC 25922 method, sterilized agar plates were inoculated with a bacterium solution (*E. coli* or *S. aureus*) with a concentration of $1-5 \times 10^8$ CFU per 150 mL of agar, and circular pieces of samples, 20 ± 5 mm in diameter, were uniformly pressed on the agar and incubated for 24 h at 37 °C. Assessment was based on the absence or presence of bacterial growth in the contact zone between the agar and the sample. The diameter of the halo (zone of inhibition) was used as a measure of the antibacterial activity, which was calculated from:

$$H = \frac{D - d}{2}$$

where H is the inhibition zone in mm, D is the total diameter of the cotton specimen and inhibition zone in mm, and d is the diameter of the specimen in mm.

In the shake flask method, antibacterial activity was investigated by placing samples (5 cm diameter) in Erlenmeyer flasks (150 mL), which were incubated with nutrient broth culture (1.0 mL) containing $1-2 \times 10^5$ CFU of bacteria for 24 h at 37 °C. The number of bacteria was indirectly measured by optical density at 625 nm in an ultraviolet–visible spectrometer, and the antibacterial activity was evaluated quantitatively with the following equation:

$$\text{Antibacterial activity (\%)} = \frac{B - A}{B} \times 100 \%$$

where B and A are the numbers of surviving cells in the unfinished cotton and finished samples, respectively.

2.6 Cytotoxicity

MTT assay was used for the cytotoxicity analysis. Samples were incubated in culture medium after sterilization by dual-antibiotics (penicillin and streptomycin). Samples were then cultured with L929 cells at a density of 1×10^5 cells/mL in 24 well plates. After incubated in the 5 % CO₂ at 37 °C for 24, 48 and 96 h, fabrics were removed. The used medium DMEM was replaced by 360 μL DMEM and 40 μL MTT solutions. After incubation for 4 h, 300 μL of DMSO was added to each well, and

the plates were shaken for 30 min at room temperature. The optical density of the formazan complex solution at 570 nm was measured with a microplate reader (ThermoFisher, USA). Pure cotton samples were set as the control group, and all experiments were conducted in triplicate.

$$\text{Cell viability (\%)} = \frac{\text{OD}_{\text{sample}} - \text{OD}_{\text{blank}}}{\text{OD}_{\text{control}} - \text{OD}_{\text{blank}}} \times 100 \%$$

2.7 Washing stability test

The washing procedure was carried out in a 1 % NaCl solution. A piece of 2×2 cm² ZnO-loaded cotton was immersed into 30 mL NaCl solution for overnight at room temperature. After immersing, the samples were rinsed in cold distilled water, and squeezed and dried at 60 °C. The concentration of ZnO loaded on the fabric was assessed using ICP-MS after different immersing cycles.

2.8 Tensile strength

Tensile strength (TS) and elongation at break (E%) were determined according to ISO 13934-1:1994.

3 Results and discussion

3.1 Morphology

SEM images of the various samples are depicted in Fig. 1, and it was noted that, apart from a few grooves, the surface of untreated cotton was generally smooth. When the cotton was finished using the silica sol (Fig. 1b), a smooth continuous film was formed on the fabric surface with a few rough clusters due to the condensation and aggregation of some sol nanoparticles. After treated with zinc precursor, the surface roughness of fiber significantly increased as shown in Fig. 1c, d since the ZnO nanoparticles were coated homogeneously throughout the fibers. The EDS analysis also confirmed the presence of zinc and other elements as shown in Fig. 2. Distinctive peaks of C, O and Zn were attributed to the cellulose matrix, and ZnO and N and Si came from the sol precursor AEAPTS. To investigate the shape and size of the produced ZnO nanoparticles, TEM analysis was used at different magnifications (Fig. 1e, f). It was observed that the particles dispersed on the surface of cotton fiber were spindle-like in shape and of 150–200 nm width and 250–300 nm length. The nanostructure of ZnO exhibits important influence on the biomedical applications [21, 22], and the spindle-like ZnO nanoparticles loaded on the cotton prepared in our paper

Fig. 1 SEM images of **a** untreated cotton, **b** AEAPTS-treated cotton, **c** ZnO-loaded cotton and **d** ZnO-loaded fiber and TEM images of **e** an individual ZnO nanoparticle and **f** magnified portion of a ZnO nanoparticle

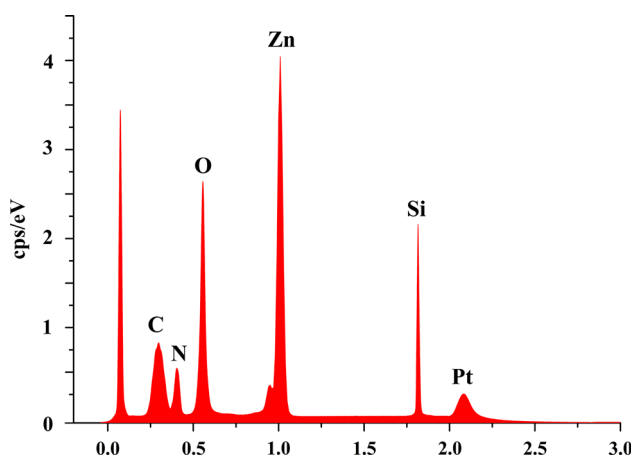
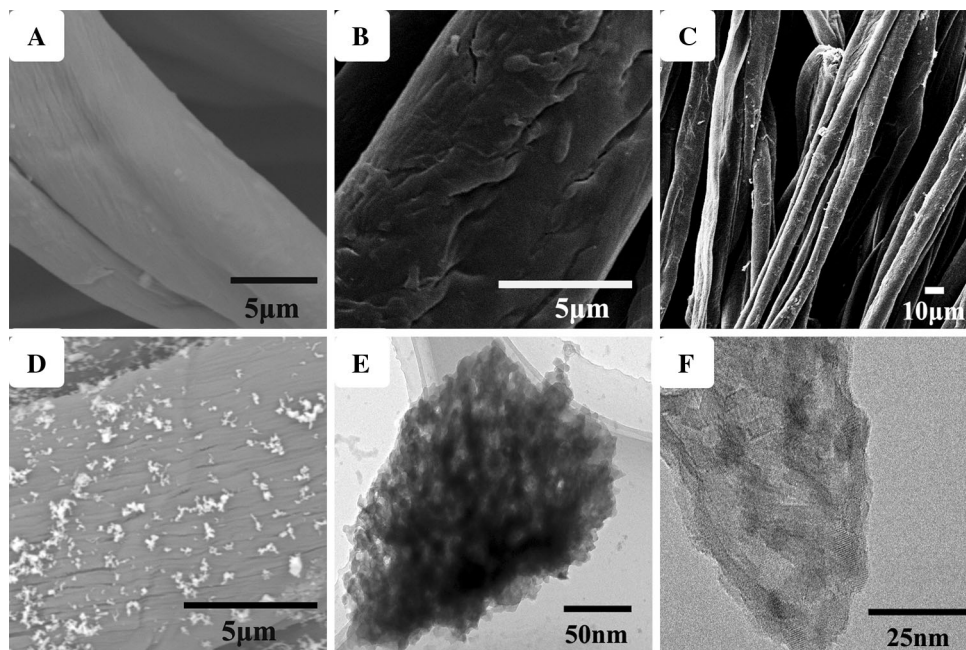


Fig. 2 EDS spectra of ZnO-loaded cotton

could be utilized in a variety of new applications in the biomedical field.

The coating process involves the in situ generation of ZnO nanoparticles and their subsequent deposition on fabrics in a one-step reaction via ultrasound irradiation based on the partly condensed AEAPTS, which could act as a reagent, template, and binder in the finishing process. The mechanism of this process was described in Scheme 1. The cotton fabric firstly absorbed AEAPTS sols to obtain the amino-containing cotton. Then, the solution involved zinc precursors turned into alkaline due to the protonation of amino groups when this treated cotton was added. Zinc nitrate was therefore converted into $\text{Zn}(\text{OH})_2$ colloids in an alkaline environment and then dissolved immediately with excessive OH^- to form $\text{Zn}(\text{OH})_4^{2-}$ as reported by Wu et al. [23]. During the ultrasonic process, $\text{Zn}(\text{OH})_4^{2-}$ could

transform into ZnO nuclei and produce ZnO nanoparticles with the $\text{Zn}(\text{OH})_4^{2-}$ as growth unit driven by local heating as a result of the collapse of sonochemical bubbles.

3.2 Further characterization

To verify the nanoparticles on the cotton fibers were indeed ZnO. Each sample was characterized by FTIR and XRD. The FTIR spectrum of pure cotton exhibited typical cellulose characteristic bands from $-\text{OH}$ at 3422 cm^{-1} and stretching vibrations of CH_2/CH groups at $2941/2912\text{ cm}^{-1}$, together with deformation bands of CH_2/CH at $1435/1375\text{ cm}^{-1}$, $\text{C}-\text{O}-\text{C}$ stretching vibrations at 1076 cm^{-1} (Fig. 3a). For AEAPTS-treated cotton in Fig. 3b; the new peak observed at 1618 cm^{-1} was ascribed to bending vibration of NH_2 . Absorption of the broad peak between 3000 and 3500 cm^{-1} was increased due to NH_2 stretching modes. Meanwhile, the characteristic peak of $\text{Si}-\text{O}-\text{Si}$ at 1058 cm^{-1} was partly overlapped with $\text{C}-\text{O}-\text{C}$ vibration. The spectrum of ZnO-loaded cotton is shown in Fig. 3c. The peak at 463 cm^{-1} was the characteristic absorption of $\text{Zn}-\text{O}$ bond, and the absorption of CH_2/CH became weak because of the coating of ZnO nanoparticles.

X-ray diffraction patterns of pure, sol-treated and ZnO-loaded cotton fabrics are presented in Fig. 4. Compared to pure cotton, AEAPTS-treated samples showed similar peaks at 14.8° , 16.6° , 22.7° and 34.2° attributed to the type I cellulose characteristics [24]. No additional peaks corresponding to other impurities were detected in the patterns, which suggested AEAPTS treatment had no influence on the crystalline nature of cotton. After loading with ZnO, which is crystalline in nature, the new peaks at

Scheme 1 Illustration for the preparation of ZnO-loaded cotton based on in situ fabrication by ultrasonic irradiation

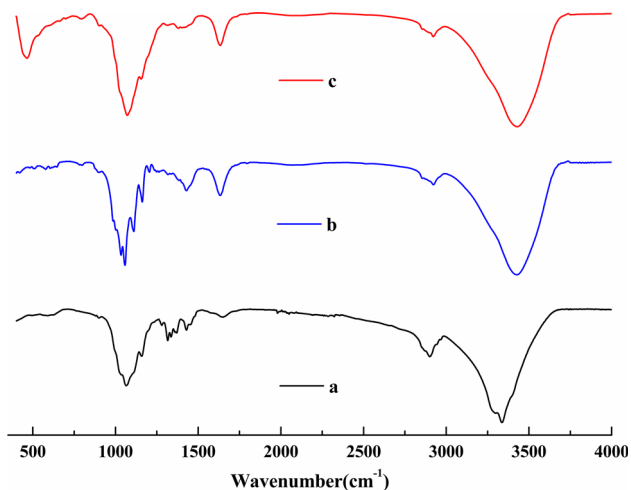
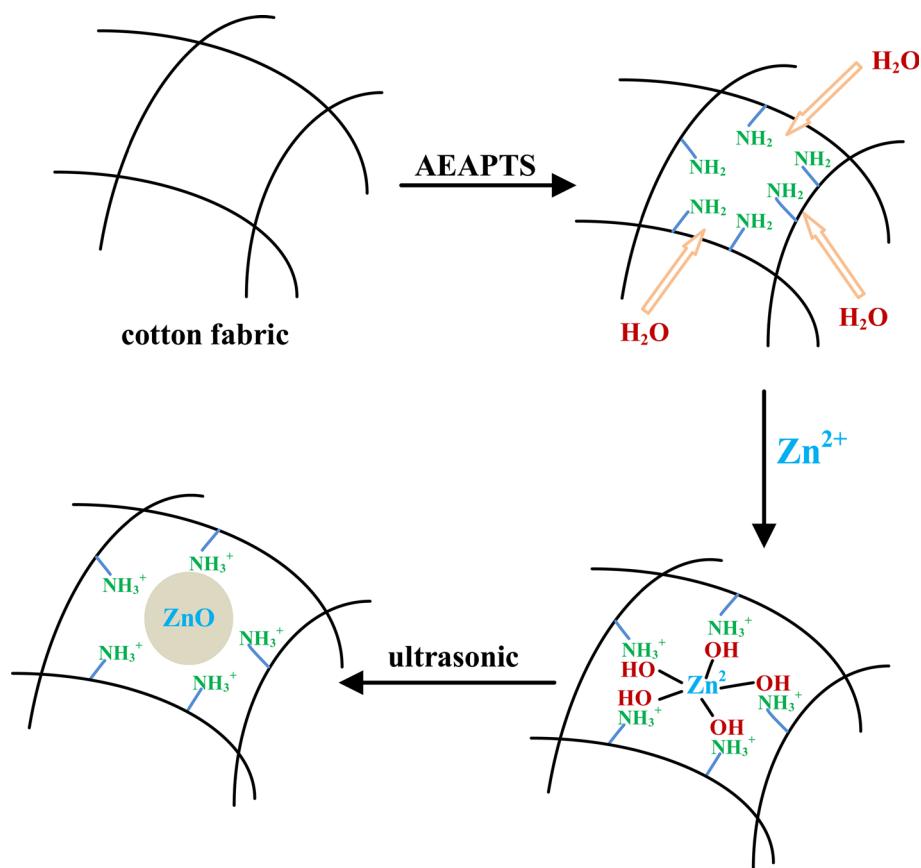


Fig. 3 FTIR spectra of (a) untreated cotton, (b) AEAPTS-treated cotton and (c) ZnO-loaded cotton

$2\theta = 31.77^\circ, 34.42^\circ, 36.25^\circ, 47.54^\circ, 56.6^\circ, 62.85^\circ$ and 67.95° were assigned to the (100), (002), (101), (102), (110), (103) and (112) reflection lines of hexagonal ZnO particles, respectively, that match very well with the hexagonal phase of ZnO (PDF: 89-7102) [25]. These results indicated that ZnO has been coated on the surface of the cotton fabric.

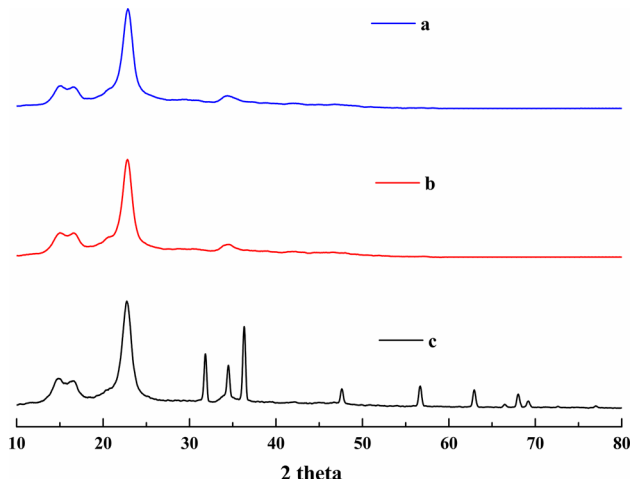


Fig. 4 XRD diffraction pattern of (a) untreated cotton, (b) AEAPTS-treated cotton and (c) ZnO-loaded cotton

TG analysis of the various samples was carried out under N_2 to investigate the thermal decomposition process and the content of ZnO. The results from the pure cotton fabric (Fig. 5a) suggested that its decomposition proceeded via three stages: initial, main and carbonization [26]. The first stage ranged from 20 to 200 °C resulted from the loss of absorbed and combined water in the

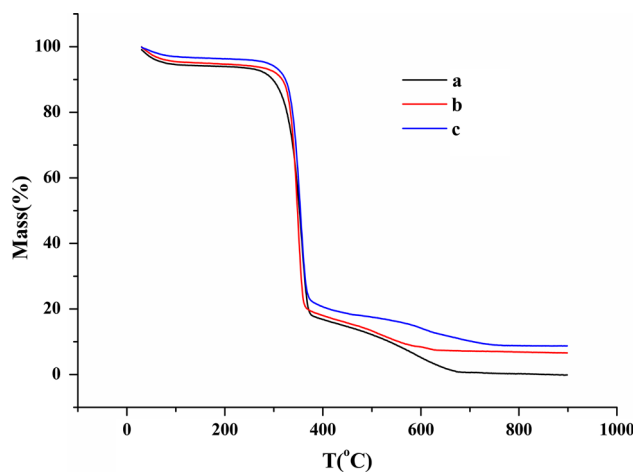


Fig. 5 TGA traces of (a) untreated cotton, (b) AEAPTS-treated cotton and (c) ZnO-loaded cotton

Table 1 UV resistance of ZnO-loaded cotton

Samples	Content of Zn (mg/g)	UPF	UVA (%)	UVB (%)
Pure cotton	0	4.18	27.21	20.35
Sol-treated cotton	0	3.42	26.46	18.12
ZnO-loaded cotton	18.26	132.45	5.21	1.37

cotton. In the second step, from 200 to 400 °C, a 60 % loss in mass was seen, and the pyrolysis was very fast and significant. L-glucose was one of the major products, together with all kinds of combustible gases. Above 400 °C, the carbonization of cellulose occurred, and the dehydration and charring reactions led to the production of glucose, water and carbon oxides until the mass loss reached nearly zero. The TG curves concerning the AEAPTS-treated and ZnO-loaded samples (Fig. 5b, c) showed the similar three stages but with lower total mass loss, which were ascribed to the undecomposed Si–O–Si and ZnO, respectively. Calculated from the difference of residual, it was estimated that the ZnO content in cotton was about 3.06 wt%. In addition, according to the concentration [$C_{Zn^{2+}}$ (mg/g)] measured by ICP-MS in Table 1, the amount of ZnO could also be calculated by the equation below:

$$\text{ZnO (wt\%)} = 0.1 \left(\frac{C_{Zn^{2+}}}{65.39} \times 16 + C_{Zn^{2+}} \right) \times 100 \%$$

where 65.39 and 16 are the molar masses of Zn and O, respectively.

It was evaluated that the ZnO content was 2.27 wt% of ZnO-loaded sample, which was a little lower than the test results in the TG analysis, possibly owing to the uneven distribution of ZnO on the cotton surface.

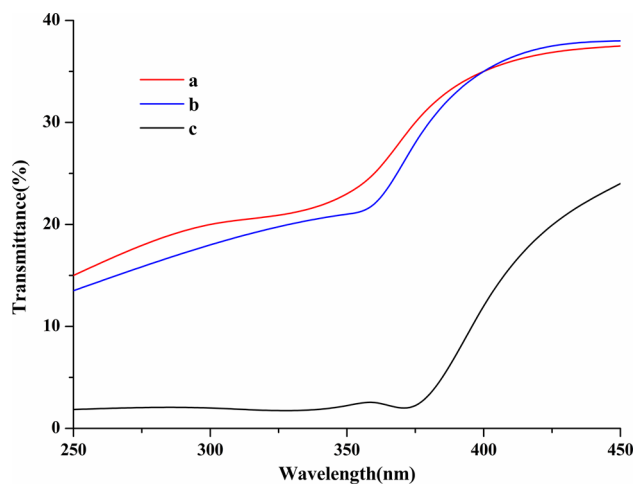


Fig. 6 UV transmittance spectra of (a) untreated cotton, (b) AEAPTS-treated cotton and (c) ZnO-loaded cotton

3.3 Ultraviolet protection properties

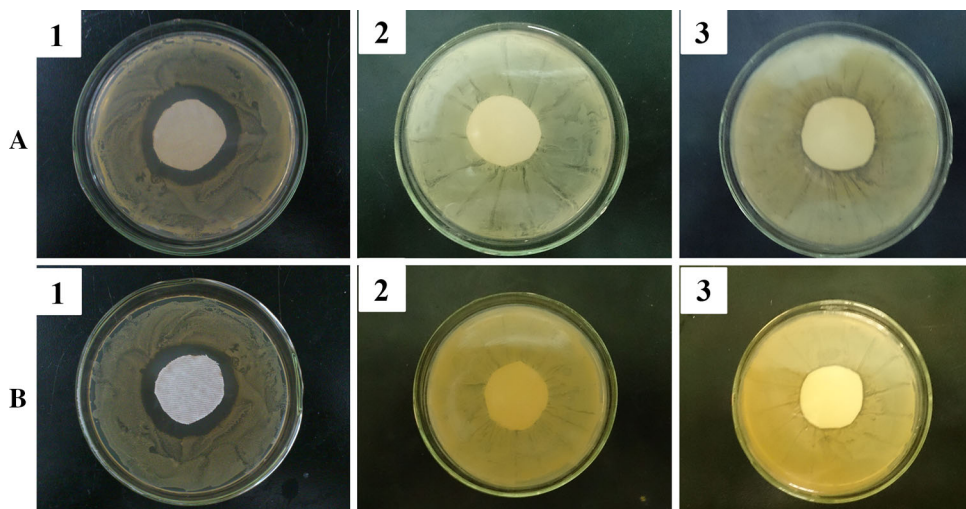
In order to investigate the UV protective properties of ZnO-loaded sample, the content of ZnO, UPF value and transmittances of UVA (320–400 nm) and UVB radiation (290–320 nm) were tested (Table 1). Generally speaking, the UV protective properties of fabrics are considered to be “good” when the UPF value is above 30 [27], that is to say, the ZnO-loaded cotton, showed enough UV resistance with UVA and UVB values of 5.21 and 1.37 %, respectively. This is due to the ZnO particles situated on the cotton surface absorbing UV radiation, and consequently the transmittances of UVA and UVB decreased correspondingly.

The UV transmission spectra of each sample are shown in Fig. 6. The sol-treated sample was no different from pure cotton in UV protection. They all presented high ultraviolet transmission and had a UPF of only about 3–4. After treating with ZnO particles, the UV transmission decreased dramatically, particularly in the UVB region (which is more detrimental to the health). The results above suggested that the ZnO-loaded cotton was very effective at blocking out ultraviolet light and providing protection to human skin.

3.4 Antibacterial activity of treated cotton

Antibacterial activity tests on the various samples were carried out against *E. coli* and *S. aureus*. Figure 7 showed the inhibition zones of fabric samples based on the qualitative bacterial test. A dense population of bacterial colonies can be seen around the pure and AEAPTS-treated cotton fabric [Fig. 7(2, 3)], which suggests no antibacterial activity for these two materials. In contrast, a clear inhibition zone of about 13 mm could be distinctly observed around the ZnO-loaded sample for both bacteria [Fig. 7(1)]. The antibacterial activity against *S. aureus* was

Fig. 7 Inhibition zone of (1) ZnO-loaded cotton, (2) AEAPTS-treated cotton and (3) untreated cotton against **a** *E.coli* and **b** *S. aureus*



98.85 % and 88.72 % for *E.coli*. This is probably because of the different sensitivity of the two bacteria to the hydroxyl radicals and oxygen radicals, which are the active species against bacteria arising from the ZnO particles [28]. When ZnO-loaded fabrics were placed in the dark, which were not illuminated by a light energy higher than the band gap energy of ZnO, there were no electron–hole pairs diffusing out to the surface of the photocatalyst. So $\cdot\text{O}$ and $\cdot\text{OH}$ would not produce to oxidize organic pollutants, and only the Zn^{2+} released from the ZnO nanoparticles could interact with the membranes of bacteria to leach out the cytoplasm and kill them. Thus, the antibacterial activity of ZnO-loaded fabrics in the dark was inferior to that with illumination, and the inhibition zone was about 11 mm.

3.5 Cytotoxicity

The cytotoxicity of sol-treated and ZnO-loaded samples was assessed using a smooth muscle cell line in Fig. 8. It was demonstrated that the viability of AEAPTS-treated sample was slightly lower than the pure one. This can be explained by the fact that the protonation of some amino groups in AEAPTS, which could interact with negatively charged cells, damages cell membranes and promotes apoptosis. ZnO-loaded cotton showed a significant effect to restrain cell proliferation as a result of the production of reactive oxygen species. Yan et al. [29] reported that the cytotoxicity induced by ZnO nanoparticles was dose-dependent, and the relative survival was below 50 % with a high dose of ZnO (0.5 mg/mL). The concentration of ZnO coated on fabric was calculated to be about 0.48 mg/mL in our paper, but higher resistance to the cytotoxicity was observed. It could be due to the ZnO particles attached to the surface of cotton and few particles entered cells via receptor-mediated endocytosis, which could induce lysis of the lysosomal membrane and ultimately causes cell death.

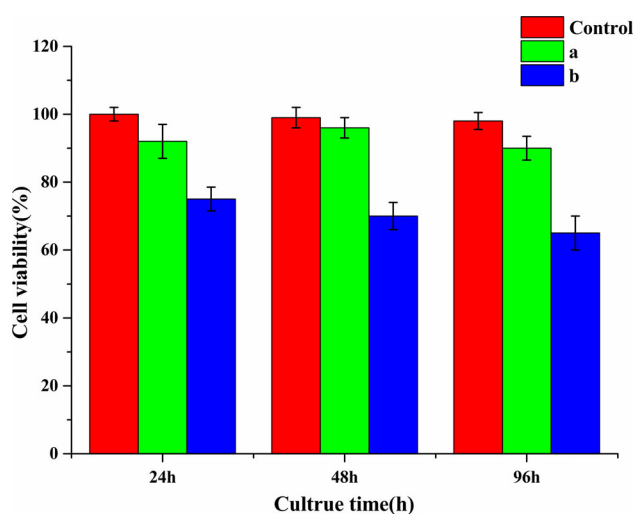


Fig. 8 Cytotoxicity studies on (a) AEAPTS-treated cotton and (b) ZnO-loaded cotton using L929 fibroblasts

3.6 Washing test

The effect of washing on various properties of ZnO-loaded samples is listed in Table 2. With an increase in washing times, ZnO content in the sample only fell by 2.85 % after 5 washing cycles, and most of the ZnO nanoparticles were still absorbed on the cotton. Also, antibacterial activity against both bacteria was above 98 and 88 %. This happened because the amino groups of AEAPTS were positively charged in solution, and there existed an electrostatic attraction with the surface oxygen atoms of the ZnO [30], thus the particles were well-attached to the treated cotton.

3.7 Tensile strength

Since the fabric tensile properties can be greatly affected by the sol-treated process, tensile strength test of the warp

Table 2 Effect of washing procedure on the properties of ZnO-loaded sample

Sample		Washing 0 time	Washing 1 time	Washing 3 times	Washing 5 times
ZnO-loaded cotton	Content of Zn (mg/g)	18.26	17.86	17.78	17.74
	Antibacterial activity (<i>E. coli</i>) (%)	88.72	88.66	88.43	88.22
	Antibacterial activity (<i>S. aureus</i>) (%)	98.85	98.84	98.72	98.69

Table 3 Tensile strength (warp direction)

	Breaking force F (N)	Breaking elongation	
		L (mm)	E (%)
1	427.5	15.69	15.69
2	350.5	14.06	14.06
3	338.5	13.08	13.08

1, pure cotton; 2, AEAPTS-treated cotton; 3, ZnO-loaded cotton

was conducted (Table 3). Treated by the sol solutions, the gel film formed by hydrolysis and condensation on the fabric gave rise to an enhanced increase in the tensile strength, but this remains inferior to the untreated cotton due to the degradation of cellulose glycosidic bonds under acid conditions and heat flux. The ZnO loaded on the cotton presented no important influence on the tensile strength, which was similar to the AEAPTS-treated sample.

4 Conclusions

In this study, we demonstrated a facile method for the growth of ZnO nanomaterials on cotton fabric under mild conditions. Morphological investigations suggested spindle-like ZnO nanoparticle could grow in the AEAPTS-treated cotton with an easy dipping method. ZnO content on cotton was 3.06 % determined by TG analysis, which was a little higher than the results calculated by ICP-MS method due to the uneven distribution of ZnO. The presence of AEAPTS on the cotton fiber was critical in growing ZnO nanomaterials in the zinc precursor solution under ultrasound-assisted treatment. AEAPTS also provided stability against washing for particles attached to the fabric. The ZnO-loaded cotton with excellent UV protective properties exhibited effective antibacterial activity against *S. aureus* and *E. coli* and moderate cytotoxicity against L929 fibroblasts. The gel coating could support the tensile strength properties of cotton fabric damaged by acid and heat treatments. This work paves the way for development of green approach to grow ZnO on flexible substrates with potentials for biomedical applications.

Acknowledgments This work was financially supported by the Natural Science Foundation of China (No. 21303014) and the Shanghai Natural Science Foundation (14ZR1401300).

References

1. E. Lombi et al., Silver speciation and release in commercial antimicrobial textiles as influenced by washing. *Chemosphere* **111**, 352–358 (2014)
2. S.T. Dubas, P. Kumlangdudsana, P. Potiyaraj, Layer-by-layer deposition of antimicrobial silver nanoparticles on textile fibers. *Colloids Surf A Physicochem. Eng. Asp.* **289**(1–3), 105–109 (2006)
3. Y. Xing, X. Yang, J. Dai, Antimicrobial finishing of cotton textile based on water glass by sol–gel method. *J. Sol-Gel Sci. Technol.* **43**(2), 187–192 (2007)
4. M.B. Radoičić et al., Influence of TiO₂ nanoparticles on formation mechanism of PANI/TiO₂ nanocomposite coating on PET fabric and its structural and electrical properties. *Surf. Coat. Technol.* **278**, 38–47 (2015)
5. M. Montazer, A. Mozaffari, F. Alimohammadi, Simultaneous dyeing and antibacterial finishing of nylon fabric using acid dyes and colloidal nanosilver. *Fibres Text. East. Eur.* **23**(2), 110 (2015)
6. J. Sawai, Quantitative evaluation of antibacterial activities of metallic oxide powders (ZnO, MgO and CaO) by conductimetric assay. *J. Microbiol. Methods* **54**(2), 177–182 (2003)
7. R. Prucek et al., The targeted antibacterial and antifungal properties of magnetic nanocomposite of iron oxide and silver nanoparticles. *Biomaterials* **32**(21), 4704–4713 (2011)
8. H.R. Jafry et al., Simple route to enhanced photocatalytic activity of P25 titanium dioxide nanoparticles by silica addition. *Environ. Sci. Technol.* **45**(4), 1563–1568 (2010)
9. S. Coyle et al., Smart nanotextiles: a review of materials and applications. *MRS Bull.* **32**(05), 434–442 (2007)
10. H.F. Moafi, A.F. Shojaie, M.A. Zanjanchi, Photocatalytic self-cleaning properties of cellulosic fibers modified by nano-sized zinc oxide. *Thin Solid Films* **519**(11), 3641–3646 (2011)
11. Z.A. Lewicka et al., The structure, composition, and dimensions of TiO₂ and ZnO nanomaterials in commercial sunscreens. *J. Nanopart. Res.* **13**(9), 3607–3617 (2011)
12. T.E. Antoine et al., Intravaginal zinc oxide tetrapod nanoparticles as novel immunoprotective agents against genital herpes. *J. Immunol.* **196**(11), 4566–4575 (2016)
13. R. Wahab et al., Self-styled ZnO nanostructures promotes the cancer cell damage and suppresses the epithelial phenotype of glioblastoma. *Sci. Rep.* **6**, 19950 (2016)
14. A. Becheri et al., Synthesis and characterization of zinc oxide nanoparticles: application to textiles as UV-absorbers. *J. Nanopart. Res.* **10**(4), 679–689 (2007)
15. N. Vigneshwaran et al., Functional finishing of cotton fabrics using zinc oxide–soluble starch nanocomposites. *Nanotechnology* **17**(20), 5087 (2006)

16. Z. Mao et al., The formation and UV-blocking property of needle-shaped ZnO nanorod on cotton fabric. *Thin Solid Films* **517**(517), 2681–2686 (2009)
17. S. Baruah, C. Thanachayanont, J. Dutta, Growth of ZnO nanowires on nonwoven polyethylene fibers. *Sci. Technol. Adv. Mater.* **9**(2), 25009 (2008)
18. A. Yadav et al., Functional finishing in cotton fabrics using zinc oxide nanoparticles. *Bull. Mater. Sci.* **29**(6), 641–645 (2006)
19. Ş.S. Ugur et al., Modifying of cotton fabric surface with nano-ZnO multilayer films by layer-by-layer deposition method. *Nanoscale Res. Lett.* **5**(7), 1204–1210 (2010)
20. W.S. Tung, W.A. Daoud, Self-cleaning fibers via nanotechnology: a virtual reality. *J. Mater. Chem.* **21**(22), 7858–7869 (2011)
21. R. Wahab et al., ZnO nanoparticles induces cell death in malignant human T98G gliomas, KB and non-malignant HEK cells. *J. Biomed. Nanotechnol.* **9**(7), 1181 (2013)
22. H. Papavlassopoulos et al., Toxicity of functional nano-micro zinc oxide tetrapods: impact of cell culture conditions, cellular age and material properties. *PLoS One* **9**(1), e84983 (2014)
23. C. Wu et al., A novel chemical route to prepare ZnO nanoparticles. *Mater. Lett.* **60**(15), 1828–1832 (2006)
24. H. Zhao et al., Studying cellulose fiber structure by SEM, XRD, NMR and acid hydrolysis. *Carbohydr. Polym.* **68**(2), 235–241 (2007)
25. I. Perelshtein et al., Antibacterial properties of an in situ generated and simultaneously deposited nanocrystalline ZnO on fabrics. *ACS Appl. Mater. Interfaces* **1**(2), 361–366 (2009)
26. P. Zhu et al., A study of pyrolysis and pyrolysis products of flame-retardant cotton fabrics by DSC, TGA, and PY-GC-MS. *J. Anal. Appl. Pyrol.* **71**(2), 645–655 (2004)
27. A. Hou, C. Zhang, Y. Wang, Preparation and UV-protective properties of functional cellulose fabrics based on reactive azobenzene Schiff base derivative. *Carbohydr. Polym.* **87**(1), 284–288 (2012)
28. G.Y. Liu et al., *Staphylococcus aureus* golden pigment impairs neutrophil killing and promotes virulence through its antioxidant activity. *J. Exp. Med.* **202**(2), 209–215 (2005)
29. D. Yan et al., Cellular compatibility of biomineralized ZnO nanoparticles based on prokaryotic and eukaryotic systems. *Langmuir* **27**(21), 13206 (2011)
30. G. Begum et al., Morphology-controlled assembly of ZnO nanostructures: a bioinspired method and visible luminescence. *Chem. Eur. J.* **14**(21), 6421–6427 (2008)